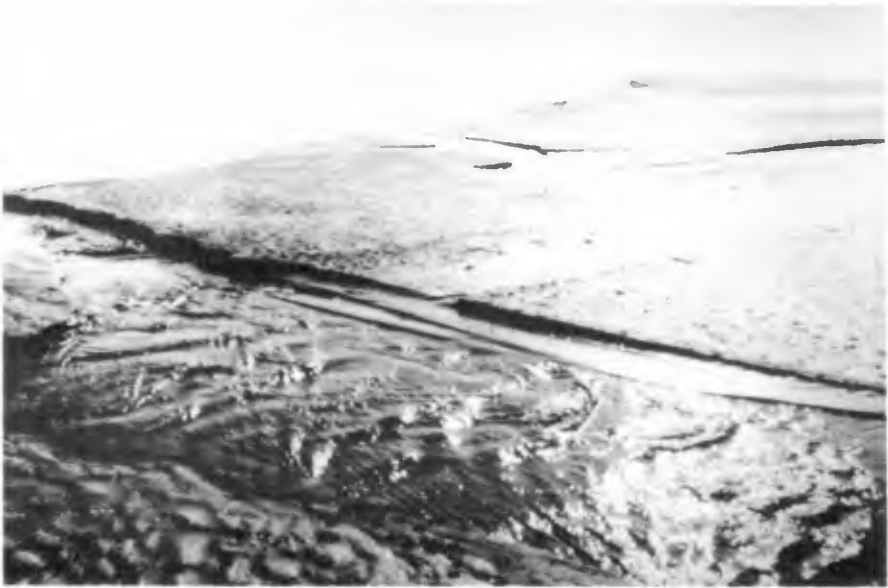


PART II

Long Waves and Storm Surges



CHAPTER 84

EVOLUTION OF INFRAGRAVITY VARIANCE DURING A STORM

Peter A. Howd¹, Joan Oltman-Shay^{1,2}, Rob Holman¹, and Paul D. Komar¹

Abstract

Data from an alongshore array of bidirectional current meters located in the surf zone were analyzed to provide estimates of the behavior of three bands of wave energy during the passage of a moderate storm. The variance in the incident wave band is found to be saturated, as is expected of depth-limited waves. The infragravity band variance is found to depend most strongly on the offshore wave height. Shear wave variance is found to be correlated with the magnitude of the measured longshore current. During a period of nearly constant high waves, the composition of the low frequency band motions ($f < 0.05$ Hz) changed dramatically. This change is thought to be related to the directional characteristics of the incident band wind waves.

Introduction

A primary interest in the study of nearshore processes has been the characterization of two frequency bands of surface gravity waves, incident wind waves ($0.05 < f < 0.33$ Hz) and infragravity waves ($f < 0.05$ Hz). The recent discovery of shear waves (Oltman-Shay, et al., 1989a; Bowen and Holman, 1989) has added additional complexity to the problem of quantifying coherent sources of energy in the nearshore.

The objective of this paper is to present data documenting the evolution of the low frequency waves during the passage of a moderate storm. The instruments used for this study were located in the trough of a nearshore bar system in approximately 1.5 m of water. In the next section we will briefly review previous work on

1. College of Oceanography, Oregon State University, OC Admin. Bldg. #104, Corvallis, Oregon, U.S.A. 97331-5503

2. Now at: Quest Integrated, 21414 68th Ave. So., Kent, Washington, U.S.A. 98032

these low frequency waves, then move on to the data collection and analysis techniques used in this study. We then present our findings and some preliminary conclusions.

Background

Infragravity waves are traditionally considered to be the surface gravity waves which result from the second order interaction of incident wind waves. The free infragravity waves can be broken into two distinct groups, a set of discrete edge wave modes which are trapped to the shoreline, and a continuum of leaky waves which reflect from the shoreline and radiate energy back out of the nearshore zone. Bounded waves, the forced displacement of the free water surface by the structure of wave groups also contribute to infragravity wave energy. Edge waves on a plane sloping beach must have alongshore wavenumbers, k , in the range $\sigma^2/g \leq |k| \leq \sigma^2/g\beta$ (where $\sigma = 2\pi f$ and $k = 2\pi/L$) satisfying the relationship $\sigma^2 = g|k| (2n+1)\beta$ (Eckart, 1951), while for leaky waves there is a continuum of alongshore wavenumbers $|k| < \sigma^2/g$ (Suhayda, 1974; Guza and Bowen, 1976).

It is important to note that measurements of infragravity waves obtained in the surf zone underestimate the maximum variance of the infragravity band for two reasons. First, while incident waves decrease in height from breaking to the shore-

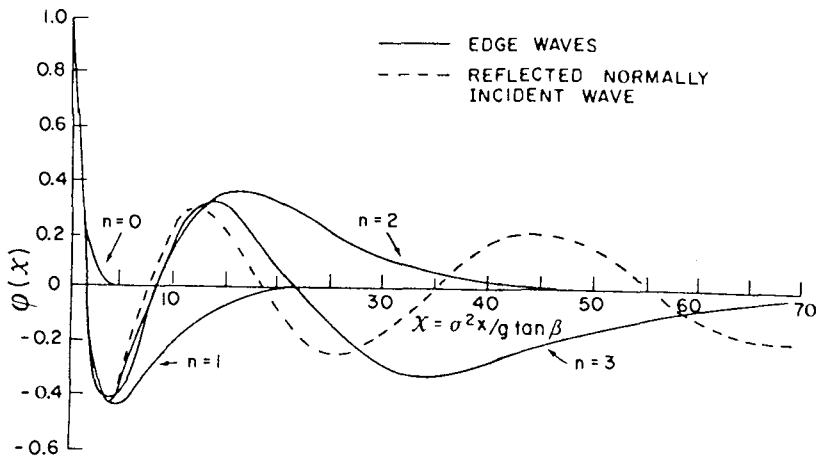


Figure 1. Cross-shore shape of the first three edge wave modes and the normally reflected leaky wave plotted versus dimensionless cross-shore distance.

line, infragravity waves have their maximum height at the shoreline and decay offshore (Figure 1). Secondly, infragravity waves have complicated cross-shore structures which contain zero crossings. Thus at any position seaward of the shore-

line, measurements are influenced not only by the offshore decay of the wave amplitudes, but by the nodal structure.

Shear waves, a new class of nearshore wave, are distinguished by large alongshore wavenumbers, well outside the range of surface gravity waves, $|k_{sw}| > \sigma^2/g\beta$ (Oltman-Shay, et al., 1989a). On the one beach studied to date, a typical energetic period is 200 s with an alongshore wavelength of 200 m. This distinctive signature permits their contribution to total current variance to be separated in alongshore wavenumber-frequency space. Bowen and Holman (1989) present a theoretical derivation of these waves as an instability of the mean longshore current which depends on the conservation of potential vorticity. The cross-shore shear of the mean longshore current provides background vorticity. Using a simple model they show there is a frequency range where a perturbation to the mean current (the shear wave) will grow exponentially at a rate which depends on the magnitude of the shear on the seaward face of the current.

Field Site and Methods

The data used for this study were collected as part of the SUPERDUCK experiment (Crowson, et al., 1988). This was a large multi-agency experiment hosted by the Coastal Engineering Research Center's Field Research Facility (FRF) in Duck, North Carolina during October, 1986. This beach is located on the mid-Atlantic coast of the United States in the center of a 100-km long barrier spit (Figure 2). The mean foreshore slope is approximately 1:10 and decreases offshore to 1:100.

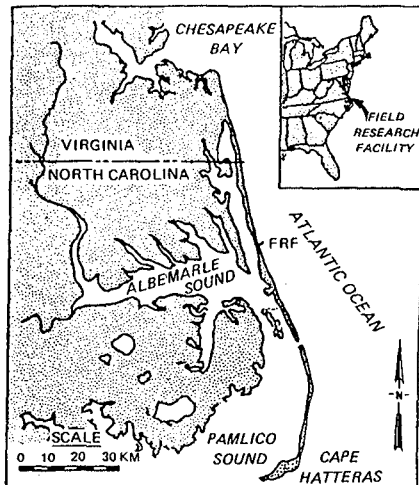


Figure 2. Location of the Coastal Engineering Research Center's Field Research Facility.

Sand bars are common, are usually three-dimensional, but become linear during

storms (Lippmann and Holman, 1990). The extreme tide range during the experiment was 137 cm.

The primary source of data for this work was an array of bidirectional electromagnetic current meters deployed approximately 55 m seaward of the mean shoreline position (Figure 3). The sampled array length was 290 m, sufficient to resolve typical wavelengths at this site. Sensors were oriented such that +V currents (alongshore) flow 'north' parallel to the beach and +U (cross-shore) currents flow offshore. All gages remained submerged at low tide. The gages were hard wired to the computer and collected at 2 Hz for four hour periods surrounding high and low water. The incident wind wave climate was sampled in 8 m depth using a 255 m long array of 9 bottom mounted pressure sensors.

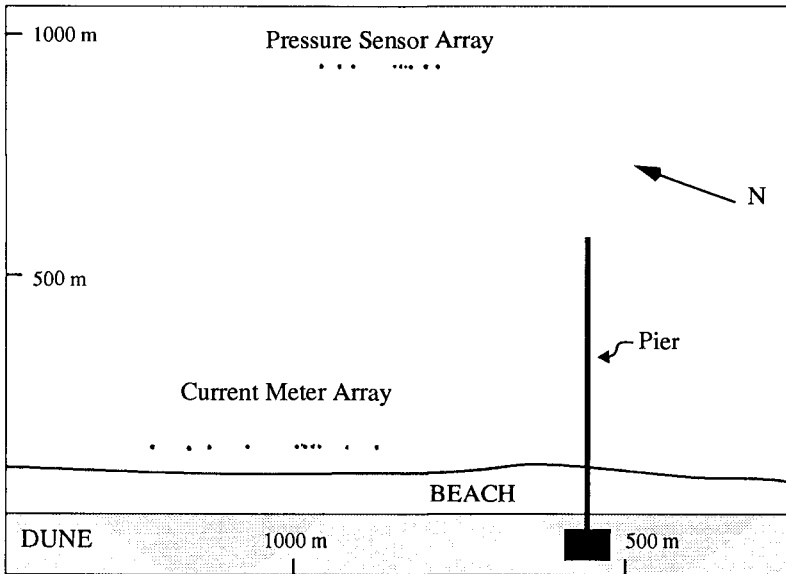


Figure 3. Plan view of the SUPERDUCK field site at CERC'S Field Research Facility in Duck, NC. Shown are the nearshore current meter array and the offshore wind wave directional array relative to the location of the pier.

A total of 37 4-hour data runs were recorded over the course of the experiment. From those, 21 were selected for further analysis on the basis of spatial homogeneity over the length of the arrays and stationarity over the 4 hour run duration. The current meter data were used to calculate the alongshore wavenumber-frequency spectra for both the cross-shore and alongshore components of flow. First each 4-hour time series was divided into 13 ensembles with 50% overlap, each 2048 s in length. The ensembles were demeaned and quadratically detrended and tapered with a Kaiser-Bessel data window. After application of an FFT, the cross-spectral constituents were calculated between all sensor pairs. Finally, alongshore wave-

number-frequency spectra were estimated using the Iterative Maximum Likelihood Estimator (IMLE) developed by Pawka (1983) and previously applied to surf zone data by Oltman-Shay and Guza (1987). The pressure sensor array in 8 m depth allowed similar alongshore wavenumber-frequency analysis.

Variance was then partitioned between the three bands in alongshore wavenumber-frequency space as shown in Figure 4. Integrated variances for each band were calculated using

$$s_{INC}^2 = \int_{0.05-k_{NY}}^{0.33-k_{NY}} \int (S(k, f)) dkdf$$

$$s_{IG}^2 = \int_0^{0.05-k_0} \int_{-k_0}^{k_0} (S(k, f)) dkdf$$

$$s_{SW}^2 = \int_0^{0.05-k_{NY}} \int_{-k_{NY}}^{k_{NY}} (S(k, f)) dkdf - s_{IG}^2$$

where s^2 is the integrated variance for each of the bands, k_{NY} is the Nyquist alongshore wavenumber of the array, k_0 is the estimated mode zero wavenumber and $S(k, f)$ is the spectral density. The subscripts refer to **INC**ident, **Infra**Gravity, and **Shear** Waves, respectively.

Results

During the 14-day period of the experiment, the root mean square (rms) wave height $(8s^2)^{1/2}$ in 8 m water depth ranged from 50 cm to over 200 cm. During the peak of the storm the wave height remained very near 200 cm for a total of 18 hours. In the surf zone, the cross-shore component of the infragravity band reached a maximum rms value of 63 cm/s and averaged 32 cm/s for the 21 4-hour runs. The alongshore component of the infragravity band had a maximum rms flow of 33 cm/s and a mean of 20 cm/s. The shear wave band had maximum rms values of 41 and 35 cm/s with means of 25 and 20 cm/s for the cross-shore and alongshore components, respectively, for the 21 runs. First we will examine the general behavior of each of the wave bands (after Howd, et al., 1991), followed by a more careful examination of two data runs from the period of high waves.

Given the position of the current meter array in the inner surf-zone shoreward of the sand bar crest, we expect to observe that the incident band was limited

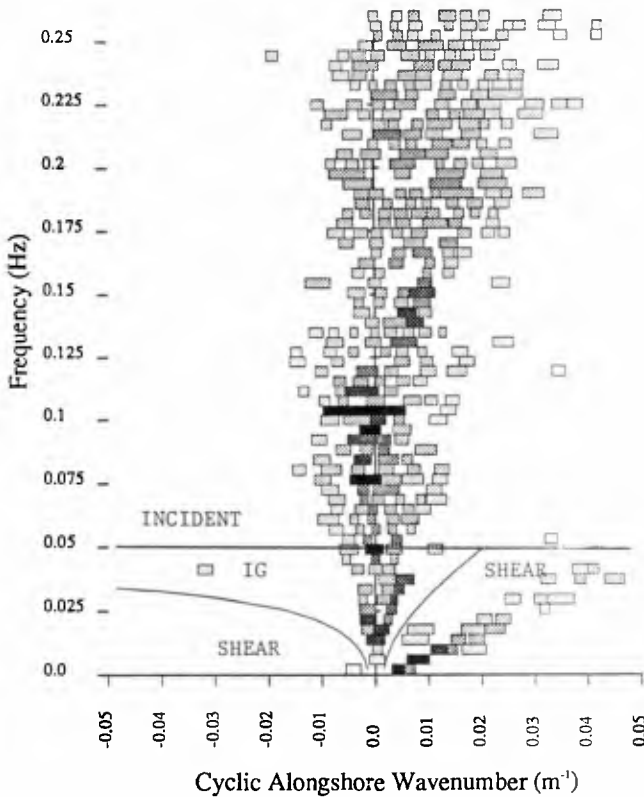


Figure 4. Cyclic alongshore wavenumber ($1/L$) vs. frequency spectrum with lines showing the bounds of each of the three wave types. The shaded boxes indicate peaks in $S(k,f)$ with the darkness indicating the higher variance. The width of the box indicates the half-power wavenumber bandwidth.

by the water depth, either at the array or further seaward at the bar crest. The strongest evidence for saturation of the incident band was the lack of statistically significant correlation (at the 95% level) between the incident wave heights at the array (calculated using linear theory) and the offshore wave height ($r^2 = 0.16$). There was however a significant correlation between the tide and the incident band wave height at the array ($r^2 = 0.80$) indicating the measurements were, as expected, a function of the water depth.

The infragravity wave motions were found to be significantly correlated with the offshore wave height ($r^2 = 0.73$ and 0.75 for the cross-shore and alongshore components, respectively). This finding is in agreement with current meter data from similar water depths on three other beaches (Holman, 1981; Guza and Thornton, 1985; Howd, et al., 1991).

Shear waves are expected to scale with the shear on the seaward face of the longshore current (Bowen and Holman, 1989), but because of the array design, no measurements of longshore current shear were available. Thus we have tested the absolute value of the mean longshore current $|\langle V \rangle|$, as a proxy for the shear. As expected from the preliminary observations of Oltman-Shay, et al. (1989a), significant correlations (95% level) were found ($r^2 = 0.25$ and 0.42 for the cross-shore and alongshore components respectively), but, as the low values suggest, considerable scatter exists in the data.

We will now compare two data runs taken during the storm. The first, taken just as the storm was reaching its peak, began at 1030 EST on October 10, 1986, and was characterized by an offshore rms wave height of 185 cm, peak period of 7.3 s and a 24.3 degree angle of incidence. The mean longshore current at the surf zone array was 160 cm/s to the south. The second run we will present was collected toward the end of the storm event and began at 1820 EST on October 11, 1986. The offshore wave height was 190 cm, the peak period was 10 s and the waves were near normally incident. The mean longshore current at the surf-zone array was 13 cm/s to the south.

Figure 5 shows the alongshore wavenumber-frequency spectra from the 8 m pressure sensor array for the two runs. To the right of each f - k spectrum is the more typical frequency spectrum (solid line). The different characteristics of the incident band are readily visible. The oblique approach of the wind waves on the 10th ($f \sim 0.125$ Hz) is clearly contrasted with the more shore-normal (at the variance peak, $f \sim 0.08$ Hz) approach on the 11th. Notice how the incident waves are clearly bounded by the line marking the relation $\sigma^2/g = k$, which is the cutoff for waves not trapped in the nearshore (i.e., they are either of deep water origin or are leaky waves reflected from the shoreline).

The infragravity band also shows surprising structure, despite the location of the sensors in 8 m of water nearly 1 km offshore. The distinctive linear trend of variance peaks from $f \sim 0.0$ to 0.10 Hz and k from 0. to 0.006 m^{-1} seen on the 10th has been shown to be the result of high mode edge waves, progressing in a southern direction (Elgar, et al., 1989; Oltman-Shay, et al., 1989b). While the high mode edge wave signature is still present on the 11th, the lowest frequencies ($f < 0.025$ Hz) appear to be more leaky in nature. There is a distinct lack of a shear wave signal at alongshore wavenumbers greater than the mode 0 dispersion curves as expected for pressure signals this far offshore (Bowen and Holman, 1989).

Figure 6 presents the alongshore wavenumber-frequency spectra computed from the alongshore component of flow in the surf-zone. As expected, the incident peaks are not visible. Most striking are the differences in the low frequency portion of the f - k spectra. On the 10th, the infragravity field was dominated by southward progressing edge waves and shear waves. The unique linear trend of the edge wave field which extends well into the incident band is unexplained, but was observed on

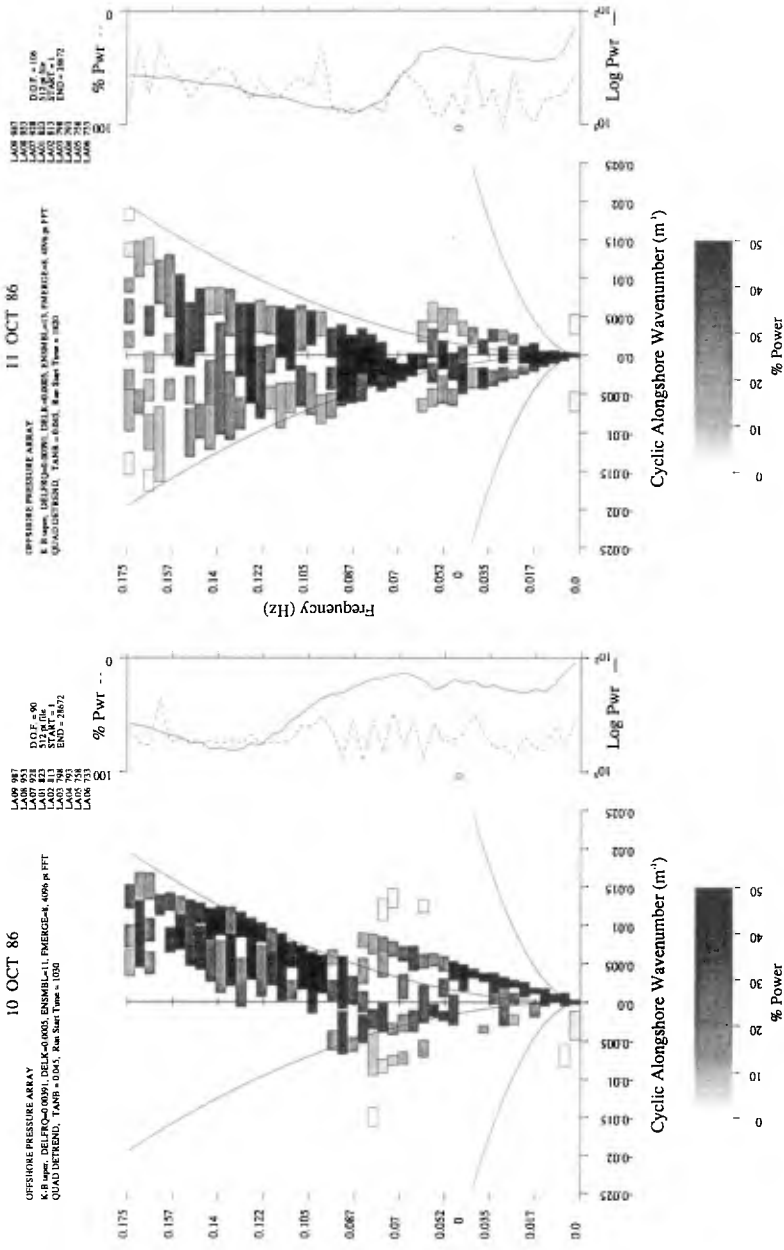


Figure 5. Frequency-alongshore wavenumber spectra from the pressure sensor array in 8 m depth. Positive wavenumbers indicate southward progressive waves. The height of the boxes indicates the frequency bandwidth, the width of the boxes indicates the half-power wavenumber bandwidth. The shading of the boxes indicates the percentage of that frequency band's variance contained in that peak. To the right of each $f-k$ spectrum is the frequency spectrum (solid line) and a representation of the percent of that frequency's variance contained in the identified peaks (dashed line). See text for interpretation of the data.

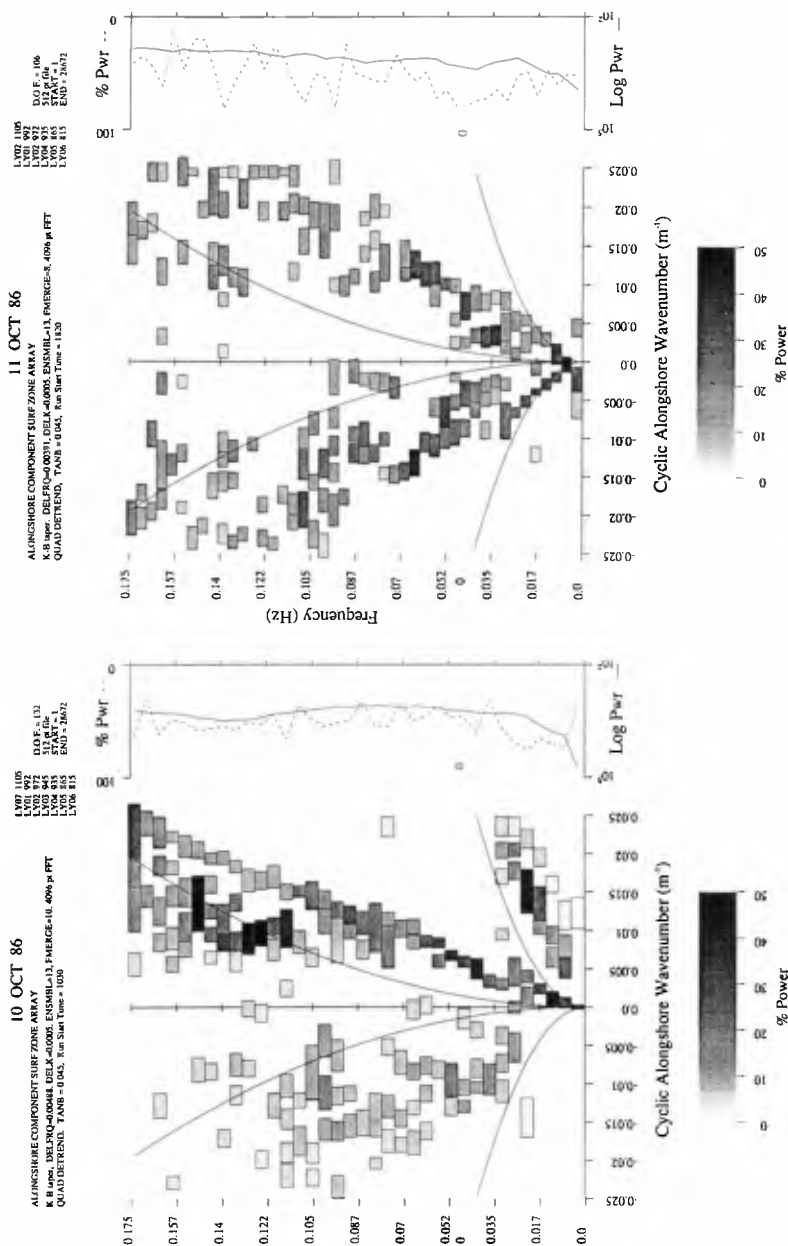


Figure 6. Frequency-wavenumber spectra calculated from the alongshore component of flow measured by the array of current meters in 1.5 m depth.

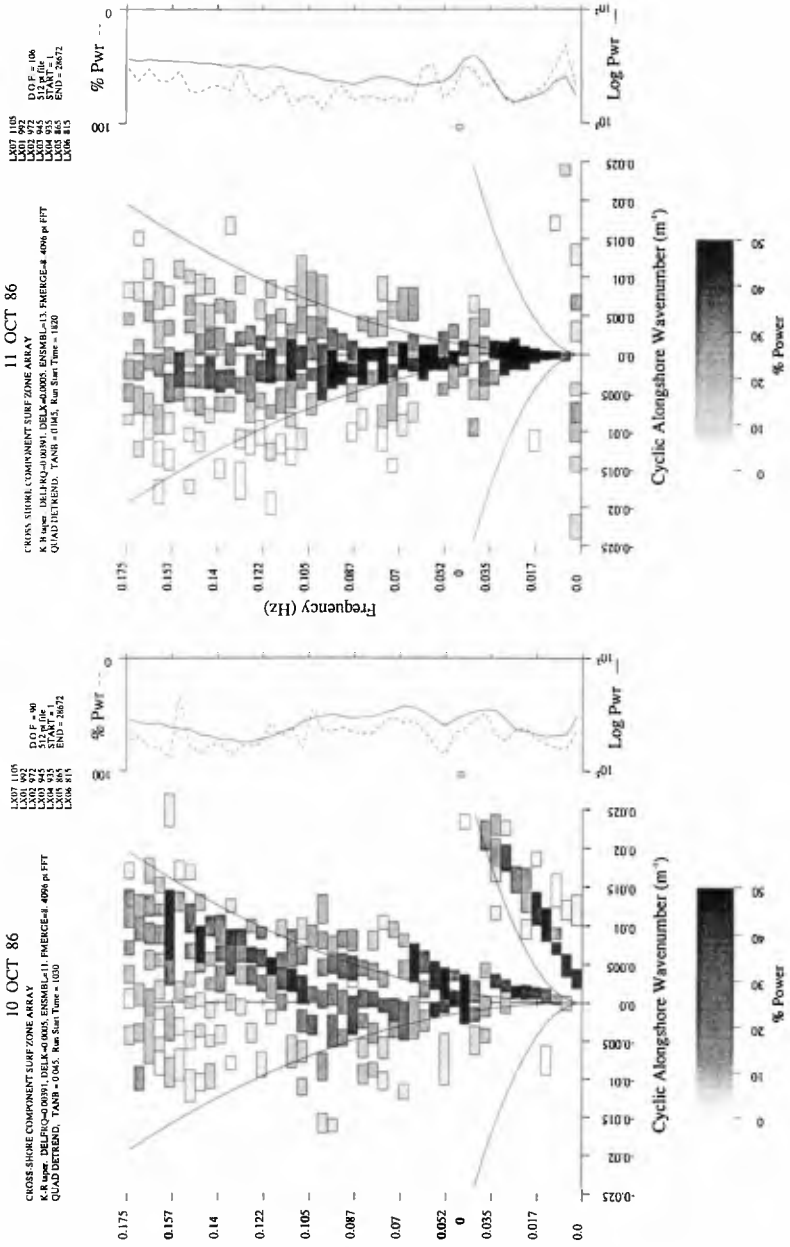


Figure 7. Frequency-wavenumber spectra calculated from the cross-shore component of flow measured by the array of current meters in 1.5 m depth.

other days with similar conditions. The rms infragravity oscillations measured 27 cm/s. The shear wave field was strong (rms oscillation of 28 cm/s) as would be expected in the presence of 160 cm/s mean currents. On the 11th, the infragravity wave field is again dominated by edge waves, but now with nearly equal contributions from the northward and southward progressive modes. The coherent structure of the shear wave band has vanished. The infragravity wave rms alongshore oscillation has remained steady at 29 cm/s while the shear wave rms value has dropped to 21 cm/s.

Figure 7 shows the equivalent spectra calculated using the cross-shore component of flow from the surf-zone sensors. The incident peaks are visible in the frequency spectra, but much less dominant than at the 8 m array (Figure 5). The differences between the low frequency motions on the two days are clear. On the 10th, not only is there a strong shear wave signal (rms oscillation of 38 cm/s), but the infragravity waves are dominated by low mode edge waves with an rms oscillation (as a band) of 36 cm/s. In contrast, on the 11th, the infragravity band is dominated by what appear to be either leaky waves or high mode edge waves. The rms oscillation of the infragravity band has nearly doubled from the 10th to 63 cm/s. As was also the case for the alongshore component of flow, the coherent structure has disappeared from the shear wave band.

While interpretation of the marked increase in the magnitude of cross-shore infragravity oscillations remains preliminary, it is safe to say that it is not due to an increase in the broad band forcing of low mode edge waves on the 11th. Oltman-Shay and Guza (1987) have shown that this should result in a simultaneous increase in the alongshore component of flow. Remembering that the alongshore rms oscillations for the two days were essentially unchanged, the increase in cross-shore oscillations is suspected to be due to an increase in the forcing of leaky waves or high mode edge waves, neither of which contribute greatly to alongshore velocity variance. A detailed study of the modal amplitudes of infragravity waves during this period is forthcoming.

Conclusions

We have used 21 4-hour data runs collected over a wide range of incident wave conditions to quantify the behavior of the alongshore and cross-shore components of wave motion for three different wave types. The incident band oscillations in the surf-zone were not significantly correlated with the offshore wave height, but were strongly correlated with the tide elevation indicating saturation due to depth limited breaking. The infragravity wave rms velocities were significantly correlated with the offshore wave height but the composition of the band appears to depend on the directional nature of the incident wind wave field. Shear waves were observed during times of strong longshore currents, but the magnitude of the current at the surf-zone array of instruments was found to be only a marginal predictor of the rms oscillations of the shear waves.

In addition there is significant evidence that the composition of the low frequency gravity wave field (edge, leaky and bound) changed considerably during the course of the storm. At the beginning of the storm when the incident waves approached the beach obliquely, the rms velocities of both components of flow in the infragravity band were nearly equal. As the angle of wave approach became nearly normal, the rms cross-shore velocity of the infragravity band grew, becoming a factor of two greater than the alongshore velocity.

Acknowledgements

We would like to thank the staff of CERC's Field Research Facility once again for the fine support they provided during the SUPERDUCK experiment. CERC also funded the deployment of the gages and the distribution of the data. The funding for the analysis of the data has been provided from grants to Oregon State University from the National Science Foundation (OCE87-11121) and the Office of Naval Research, Coastal Sciences Program (N00014-87-K0009).

References

- Crowson, R., W. Birkemeier, H. Klein, and H. Miller, 1988, SUPERDUCK near-shore processes experiment: Summary of studies CERC Field Research Facility, *U.S. Army Tech. Report CERC-88-12*.
- Bowen, A.J. and R.A. Holman, 1989, Shear instabilities of the mean longshore current; I. Theory, *J. Geophys. Res.* 94: 18032-18041
- Elgar, S., J. Oltman-Shay, and P. Howd, 1989, Observations of infragravity frequency long waves; I. Coupling to wind waves, *EOS, Trans. Am. Geophys. Union*, 70:1133.
- Guza, R. and E. Thornton, 1985, Observations of surf beat, *J. Geophys. Res.*, 90:3161-3172.
- Guza, R. and A.J. Bowen, 1976, Resonant interactions for waves breaking on a beach, *Proc., 15th ICCE* 560-579.
- Holman, R.A., 1981, Infragravity energy in the surf zone, *J. Geophys. Res.*, 86:6442-6450.
- Howd, P.A., J. Oltman-Shay, and R.A. Holman, accepted, Wave Variance Partitioning in the Trough of a Barred Beach, *J. Geophys. Res.*
- Lippmann, T.C. and R.A. Holman, 1990, The spatial and temporal variability of sand bar morphology, *J. Geophys. Res.*, 95:11575-11590.

- Oltman-Shay, J. and R.T. Guza, 1987, Infragravity wave observations on two California beaches, *J. Physical Oc.*, 17: 644-663.
- Oltman-Shay, J., P.A. Howd, and W.A. Birkemeier, 1989a, Shear instabilities of the mean longshore current; II. Field observations, *J. Geophys. Res.* 94: 18031-18042.
- Oltman-Shay, J., S. Elgar, and P. Howd, 1989b, Observations of infragravity frequency long waves; II. Comparison with a 2-D wave group generation model, *EOS, Trans. Am. Geophys. Union*, 70:1133.
- Pawka, S., 1983, Island shadows in wave directional spectra, *J. Geophys. Res.*, 86:2579-2591.
- Suhayda, J., 1974, Standing waves on beaches, *J. Geophys. Res.* 72: 3065-3071.